Mon. Not. R. Astron. Soc. **378,** 221–230 (2007) doi:10.1111/j.1365-2966.2007.11768.x

Selection of ThAr lines for wavelength calibration of echelle spectra and implications for variations in the fine-structure constant

M. T. Murphy,[1⋆] P. Tzanavaris,[2,3] J. K. Webb[2] and C. Lovis[4]

[1]*Institute of Astronomy, University of Cambridge, Madingley Road, Cambridge CB3 0HA*
[2]*School of Physics, University of New South Wales, Sydney, NSW 2052, Australia*
[3]*Institute of Astronomy and Astrophysics, National Observatory of Athens, I. Metaxa & V. Pavlou, 152 36 Penteli, Greece*
[4]*Observatoire de Genève, 51 Ch. des Maillettes, 1290 Sauverny, Switzerland*

Accepted 2007 March 20. Received 2007 March 15; in original form 2006 November 29

ABSTRACT

Echelle spectrographs currently provide some of the most precise and detailed spectra in astronomy, the interpretation of which sometimes depends on the wavelength calibration accuracy. In some applications, such as constraining cosmological variations in the fundamental constants from quasar absorption lines, the wavelength calibration is crucial. Here we detail an algorithm for selecting thorium–argon (ThAr) emission lines for wavelength calibration which incorporates the properties of both a new laboratory wavelength list and the spectrograph of interest. We apply the algorithm to the Very Large Telescope Ultraviolet and Visual Echelle Spectrograph (UVES) and demonstrate a factor of $\gtrsim$3 improvement in the wavelength calibration residuals (i.e. random errors) alone. It is also found that UVES spectra calibrated using a previous, widely distributed line-list contain systematic $\pm$30–75 m s^{-1} distortions of the wavelength scale over both short and long wavelength ranges. These distortions have important implications for current UVES constraints on cosmological variations in the fine-structure constant. The induced systematic errors are most severe for Mg/FeII quasar absorbers in the redshift range $1.2 \lesssim z_{\rm abs} \lesssim 2.3$, with individual absorbers studied by recent authors containing systematic errors up to four times larger than quoted statistical errors.

Key words: atomic data – line: identification – techniques: spectroscopic – atlases – quasars: absorption lines.

1 INTRODUCTION

Echelle spectrographs are the most common instrument for recording high-dispersion astronomical spectra. Since many echelle diffraction orders can be cross-dispersed and thereby recorded simultaneously on rectangular-format media (e.g. modern CCDs), more-or-less continuous wavelength coverage over much of the optical range can be achieved whilst maintaining high resolving power[1]. To fully exploit the velocity precision available in high-resolution spectra, precise wavelength calibration over much of the optical range is required. This is now usually done by comparison with exposures of a thorium–argon (ThAr) hollow-cathode emission-line lamp (e.g. Breckinridge, Pierce & Stoll 1975).

After Meggers (1957) first suggested that Th transitions might act as reliable wavelength standards, many authors (e.g. Giacchetti, Stanley & Zalubas 1970) measured Th laboratory wavelengths and confirmed their suitability for such purposes. There are several reasons the ThAr spectrum has proven an enduring standard for astronomical spectroscopy. (i) Most optical ThAr transitions have measured laboratory wavelengths, most of which are resistant to pressure and Stark shifts. (ii) Th has one stable isotope and terrestrial Ar is almost entirely composed of ^{40}Ar (Rosman & Taylor 1998). Also, both Th and ^{40}Ar have even nuclei. Therefore, no unresolved isotopic or hyperfine structure in the ThAr lines is expected. (iii) Most ThAr lines are unresolved at most practical resolving powers, that is, $R \lesssim 150\,000$. (iv) The ThAr line-density is high, $\gtrsim$1 line per Å, over most of the optical range. (v) ThAr lamps are fairly cheap, are commercially available and have lifetimes of typically $\gtrsim$1 yr. Other calibration sources include iodine absorption cells (e.g. Marcy & Butler 1992) but these degrade the object signal and can only be used over a comparatively short wavelength interval (typically $\sim$5000–6500 Å). Another, potentially ultrastable, absolute calibration system might be based on the new technology of laser frequency combs (Murphy et al. 2007a), a possibility now under development.

Despite the distinct advantages, there are, however, several drawbacks to using ThAr spectra for wavelength calibration. First, different ThAr lines have widely different intensities, far beyond the typical dynamic range of modern CCDs (i.e. a factor of $\sim$50 000).

⋆E-mail: mim@ast.cam.ac.uk

[1] Resolving power $R \equiv \lambda/\mathrm{FWHM}$, where FWHM is the instrumental profile's full width at half-maximum.

Secondly, the wavelength distribution of lines is highly non-uniform; it turns out that *most* ThAr lines are blended with relatively strong nearby lines, even at $R \lesssim 150\,000$. It is therefore important to carefully select which ThAr lines are to be used when calibrating echelle spectra. This task is complicated by the fact that a given line's intensity (relative to other lines) varies from lamp to lamp and even within the one lamp over time. ThAr lines arise from a variety of Th and Ar ionization states and so, as the lamp ages and/or the operating current and pressure are varied, the relative strengths of different lines can change. Thus, ideally, detailed selection of ThAr lines for wavelength calibration is best carried out separately for each ThAr exposure. However, in practice, most spectrograph-specific data reduction pipelines carry out only simple and minimal line selection, thereby assuming that a detailed pre-selection of lines has already been carried out. That is, for most practical purposes, it suffices to have a ThAr line-list pre-selected for the spectrograph of interest.

In this paper we detail an algorithm to pre-select ThAr lines for any echelle spectrograph and we apply the algorithm to the Ultraviolet and Visual Echelle Spectrograph (UVES) on the European Southern Observatory's (ESO's) Very Large Telescope (VLT) on Cerro Paranal, Chile. ESO have already pre-selected ThAr lines to calibrate UVES and the line-list is included with the ESO pipeline for UVES data reduction. Their selection derives from the results of De Cuyper & Hensberge (1998, hereafter DCH98) who constructed simulated ThAr emission spectra based on line tables in the literature. DCH98 report 'effective' wavelengths for selected ThAr lines given the expected degree of line blending based on the relative line intensities in the literature. The effective wavelengths therefore depend on resolution; the ESO list is based on the $R = 100\,000$ results of DCH98.[2] However, the ESO list is not identical to the DCH98 list and seems to include >500 lines which were rejected by DCH98 because no effective wavelengths could be found. Furthermore, all wavelengths are only given to three decimal places (in units of Å) and, in many cases, the wavelengths were *truncated*, rather than rounded, from four decimal places.

Such treatment of the ThAr line-list can cause non-negligible systematic effects in several applications. In this paper we focus on the effects it has had on current constraints on cosmological variations in the fine-structure constant, $\alpha_{\rm em}$, derived from VLT/UVES quasar absorption spectra. If $\alpha_{\rm em}$ were different in the high-redshift absorption clouds, the relative wavelengths of different metal-line transitions would differ from those observed in laboratories on Earth. This effect provides a precise observational probe of possible variations in $\alpha_{\rm em}$ over cosmological time- and distance-scales called the 'many-multiplet' (MM) method (Dzuba, Flambaum & Webb 1999; Webb et al. 1999). Analyses of a large sample of quasar spectra from the Keck High-Resolution Echelle Spectrograph (HIRES) have so far provided the first evidence for variation in $\alpha_{\rm em}$ (Webb et al. 1999; Murphy et al. 2001b; Webb et al. 2001; Murphy, Webb & Flambaum 2003) with the most recent results indicating a smaller $\alpha_{\rm em}$ in the absorption clouds at the fractional level of $\Delta\alpha/\alpha = (-0.57 \pm 0.11) \times 10^{-5}$ (Murphy et al. 2004). Clearly, such a potentially fundamental result must be refuted or confirmed with many different telescopes and spectrographs. Some first attempts with VLT/UVES have now been made (e.g. Chand et al. 2004, 2006; Levshakov et al. 2006), generally yielding no variation in $\alpha_{\rm em}$. While detailed analyses of HIRES ThAr spectra have shown no signs of strong systematic errors (Murphy et al. 2001a, 2003), no similar general assessment has yet been made for the bulk of the UVES constraints on $\Delta\alpha/\alpha$. Given the errors in the ESO ThAr line-list, it is imperative to do so.

This paper is organized as follows. In Section 2 the various ThAr transition tables in the literature are combined according to their different strengths and weaknesses. Section 3 details the line selection algorithm. Section 4 describes the final ThAr line-list for use in calibrating VLT/UVES spectra and shows the distortions of the wavelength scale introduced by the errors in the ESO line-list. Section 5 assesses the general implications these distortions have for current UVES constraints on a varying fine-structure constant.

2 SYNTHESIS OF EXISTING TH AND AR LINE-LISTS

Before selecting which ThAr lines are to be used to calibrate UVES, we first require a list of laboratory wavelengths for as many features as possible which appear in measured UVES ThAr lamp spectra. Most features, especially below 7000 Å, are either known to be due to Th or are unidentified (but probably due to Th), while ∼7 per cent of the features are from Ar and <1 per cent are from 'contaminant' species such as Na I, Mg I, Ca II and Fe I. The Th and Ar lines, and even some of the contaminant lines, are catalogued in various atlases derived from painstaking (but usually rather old) laboratory work. These atlases provide our starting point. However, every ThAr lamp gives a somewhat different spectrum and there always appear additional lines which cannot be found in any atlas, even as 'unidentified' lines. These are probably due to additional contaminant ions and molecular species in the lamp. This means that our prior knowledge of the ThAr spectrum from any given lamp is, at best, incomplete, thereby necessitating the selection procedure detailed in the next section.

There is no single ThAr atlas covering the whole wavelength range of UVES, ∼3030–10 540 Å. However, there is one atlas of Th lines only which does cover this range, Palmer & Engleman (1983, hereafter PE83). The PE83 absolute velocity precision varies from ∼15 to ∼120 m s^{-1} depending on the line intensity. PE83 identify a large number of Th I, Th II and Th III lines in their spectrum but a large number of unidentified lines remain, most of which are probably due to Th. Furthermore, on comparison with real ThAr lamp spectra, one notices that there are still several thousand lines which cannot be accounted for by Ar or contaminant species.

Very recently, Lovis & Pepe (2007, hereafter LP07) used a large library of ThAr spectra taken over one month with the High Accuracy Radial Velocity Planet Searcher (HARPS) spectrograph on the 3.6-m ESO telescope to improve the measurement precision of many ThAr lines, at least over the HARPS wavelength range of 3785–6915 Å. They identified in their spectra lines from the PE83 atlas which showed no strong wavelength variations with time and obtained line positions with a root-mean-square variation (rms) of typically 5–10 m s^{-1}. Thus, while bootstrapping their overall wavelength scale to that of PE83, they were able to correct the wavelengths of individual PE83 lines, especially weaker lines. Moreover, they were able to measure the wavelengths of all other features in their ThAr spectra, again at the 5–10 m s^{-1} precision level. They removed from their list lines which saturated their CCD, (very few) lines which appeared in the PE83 catalogue but which were not detected in the HARPS spectra and, most importantly, they removed lines which were either closely blended with other lines at the HARPS resolving power of $R = 120\,000$ or were observed to change position with time. The latter indicates either that the line experiences significant shifts with changing lamp pressure or current or that the line is actually a blend and that the relative intensities

[2] http://www.eso.org/instruments/uves/tools/tharatlas.html

of the blended lines varies with changing lamp conditions. In this work we use all lines from the LP07 atlas excluding those which have relative wavelength errors amounting to $>120\,\mathrm{m\,s^{-1}}$; a total of 8219 out of 8442 lines are used from LP07.

The LP07 catalogue ranges from 3785 to 6915 Å. In selecting lines for use in calibrating UVES, we use the PE83 line-list for Th and contaminant lines outside this range. However, it is important to begin with a list which includes the known Ar lines as well so that (i) the maximum number of known blends can be identified and removed and (ii) the maximum number of lines are available for calibrating UVES. Three Ar line-lists exist with similar wavelength precision – Norlén (1973, hereafter N73), Whaling et al. (1995, hereafter W95) and Whaling et al. (2002, hereafter W02) – each of which has different advantages and disadvantages. The N73 atlas contains both Ar I and Ar II lines whereas W95 contains Ar II lines only and W02 contains Ar I lines only. Fewer lines are listed by N73 compared to W95 and W02 since the N73 experiment was less sensitive to weak lines. The velocity precision achieved by N73 for the Ar I lines is better than that of W02 but the velocity precision of the W95 Ar II lines is better than that of N73. Finally, there is a calibration difference such that the Whaling et al. wavenumbers are larger than those of Norlén by a factor of $S_{\mathrm{NW}} = 1 + 6.8 \times 10^{-8}$. The calibration given by Whaling et al. should be more reliable since it uses calibration lines in the same recorded spectra as the Ar II lines. Therefore, we use the Whaling et al. calibration scale in synthesizing the Ar line-lists.

The different lists of Ar I and Ar II lines are combined in the following ways. We do not consider the Ar III lines from W95 since there are very few of them and since their wavelengths have larger uncertainties (W. Whaling, private communication).

(i) Ar I: Following the recommendation in W02 we used N73 wavenumbers (scaled by S_{NW}) when available, otherwise W02 values were used. For N73 lines, the intensity scale of N73 was used as recast by DCH98 on to a logarithmic scale. For W02 lines, the W02 intensity scale was used.

(ii) Ar II: W95 wavelengths were used here since W95 claim that they are relatively insensitive to pressure shifts and that their values are more precise than those of N73. In the few cases where N73 reports an Ar II line that W95 doesn't, the N73 wavelength (scaled by S_{NW}) was used. For W95 lines the W95 intensity scale was used (this is the same as the W02 intensity scale). For N73 values, the intensity scale of N73 was used as recast by DCH98 on to a logarithmic scale. Note that N73 uses the intensity scale of Minnhagen (1973) for Ar II lines above air wavelengths of $\lambda_{\mathrm{air}} = 7600$ Å and below $\lambda_{\mathrm{air}} = 3400$ Å. This subtlety is neglected in the considerations below.

After combining the LP07, PE83, N73, W95 and W02 lists in the above way we obtain the list hereafter referred to as LPWN. Note from the above that the intensity scales for each species (e.g. Th I, Ar I, Ar II) are different and that the relative intensities of lines from different species depend on many factors such as lamp pressure and current and the relative partial pressures of Th and Ar gas used.

3 THAR LINE SELECTION

One should not simply use the above line-list, LPWN, to calibrate UVES spectra because of the potential for line-blending. The Fourier transform spectra of PE83, N73, W95 and W02 and the HARPS spectra of LP07 all have resolving powers $R \geqslant 120\,000$ whereas the UVES resolving power is typically 35 000–70 000 and possibly as high as 110 000. Therefore, a major part of the line selection that follows is the rejection of 'close' blends. The concept of 'close' clearly depends on the relative intensities of the blended lines and so it is necessary to put all lines in LPWN list on to the one intensity scale typical of UVES ThAr spectra. Furthermore, since there are always additional unknown lines in measured ThAr spectra, a given ThAr line can only be used for calibration if it is *measured* to be reliable in the UVES ThAr spectrum. For these reasons we have constructed a UVES ThAr spectrum for use in the line selection process.

3.1 UVES ThAr spectrum

ThAr spectra taken as part of regular UVES maintenance activities with a 0.6-arcsec slit and no CCD rebinning were retrieved from the ESO Science Archive. Exposures from several different standard UVES wavelength settings[3] (346, 437, 580, 600, 760 and 860-nm) were used to provide complete wavelength coverage, with the exception of three small echelle order gaps redwards of 10 000 Å (10 084.43–10 085.93, 10 252.42–10 256.95 and 10 426.10–10 433.76 Å). The UVES pipeline[4] was used to extract and wavelength calibrate the data. Several modifications to the pipeline, which will be reported elsewhere, were made to improve object extraction and wavelength calibration. The data were redispersed to a log-linear wavelength scale using UVES POPLER,[5] code specifically written to redisperse and combine UVES data from multiple wavelength settings. Overlapping regions of spectra were cut away so that only one raw exposure contributed to the final spectrum at any given wavelength. No effort was made to flux-calibrate the final spectrum and the blaze-function of the echelle grating was still evident in the combined spectrum. However, our results from the intensity rescaling in the next section demonstrate that this is a minor consideration. The final spectrum has a resolving power of $R \approx 70\,000$ and the log-linear dispersion is set to $1.75\,\mathrm{km\,s^{-1}}$.

3.2 ThAr line selection algorithm

The above line-list, LPWN, is treated as the input catalogue to the following algorithm for selecting a final list for calibration of UVES. We make three passes through the algorithm, refining at each pass the line-list used to calibrate the UVES ThAr spectrum and other parameters specified below. Figs 1–7 pertain to the final pass through the algorithm.

(i) Wavelength calibrating the UVES ThAr spectrum: The procedure in Section 3.1 for constructing the UVES ThAr spectrum requires an input line-list for the wavelength calibration stage. At the first pass we use the line-list provided by ESO with the UVES pipeline. At the second and third passes the output from the previous pass through the algorithm is used. Note that the line-list used at the first pass is irrelevant; only an approximate wavelength scale needs to be established initially and this is greatly refined by subsequent passes through the algorithm.

(ii) Gaussian fitting: Each line in the input list LPWN is searched for in the UVES ThAr spectrum and fitted with a Gaussian. The fit includes the 13 pixels centred on the pixel with maximum intensity. A first-guess continuum level is defined by averaging the first and last 2 pixels in the window. A first-guess continuum slope is defined from the difference between these averages. A first-guess

[3] The 760-nm exposure was taken on 2005 March 21. All other exposures were taken on 2004 February 11.
[4] http://www.eso.org/projects/esomidas
[5] http://www.ast.cam.ac.uk/~mim/UVES_popler.html

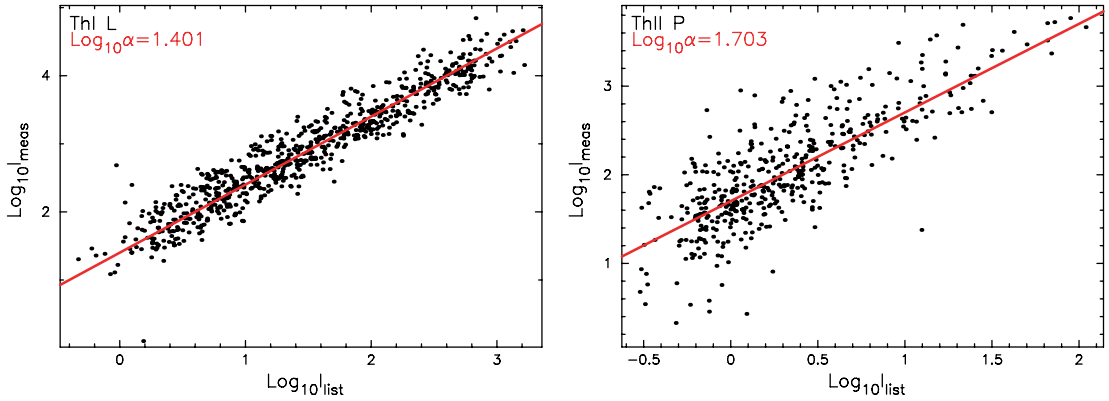

Figure 1. Examples of the intensity scaling procedure. Measured and catalogued intensities, $I_{\rm meas}$ and $I_{\rm list}$, respectively, for unblended lines from each category – Th I from LP07 and Th II from PE83 in this figure – are compared to derive the scalefactor, α. All lines from that category are then scaled by α to the UVES intensity scale.

amplitude is defined as the maximum intensity minus the continuum level. A first-guess width is defined from the velocity difference between the first and last pixels which have intensities less than the continuum plus half the first-guess amplitude. The first-guess central velocity is calculated as the intensity-weighted velocity of the 3 central pixels. A five-parameter Gaussian fit is performed and the best-fitting parameters are used in the subsequent steps of the line selection algorithm. The initial guesses and Gaussian fitting procedure are identical to those we used in our modifications to the UVES pipeline.

(iii) Intensity rescaling: The different Th and Ar atlases combined above have different intensity scales. Furthermore, one would not expect to find the same relative intensities for lines of different ionization stages (e.g. Ar I and Ar II) in the laboratory and UVES spectra since the ThAr lamps will have had different operating conditions (e.g. pressure, current, etc.). We therefore aim to place all lines from the different ionic species (i.e. Th I/II/III, Ar I/II, contaminant and unidentified species) from each different intensity scale (i.e. LP07, PE83, N73 and W95/W02) on a single intensity scale directly related to the UVES ThAr spectrum. First, any pairs of lines within 13 km s^{-1} of each other are removed from the input line-list LPWN. For each 'category' of line – for example, Th I from LP07, Th I from PE83, Ar II from LP07, Ar II from W95 etc. – the catalogued intensities are compared with those measured from the Gaussian fits performed on the UVES ThAr spectrum. The median ratio of measured and catalogued intensity, α, is defined as the scalefactor. All lines from this category are then scaled to the UVES intensity scale by multiplying their catalogued intensities by α. Two examples of this process are shown in Fig. 1. Fig. 2 shows all lines from all categories placed on the UVES intensity scale.

(iv) Blend removal: If, when Gaussian-fitting a single line, another weaker blending line is present but ignored in the fit, then the centroid returned from the fit will be shifted towards the blending line. The magnitude of the shift will depend not only on the velocity separation between the two lines, $\Delta\, v_{\rm sep}$, but also on the relative intensities of the two lines, I_2/I_1. When the two lines are not resolved from each other, it is easy to estimate the velocity shift: the new centroid wavelength is approximately the intensity-weighted mean wavelength of the two blended lines,

$$\lambda_{\rm c} \approx \frac{I_1\lambda_1 + I_2\lambda_2}{I_1 + I_2}. \quad (1)$$

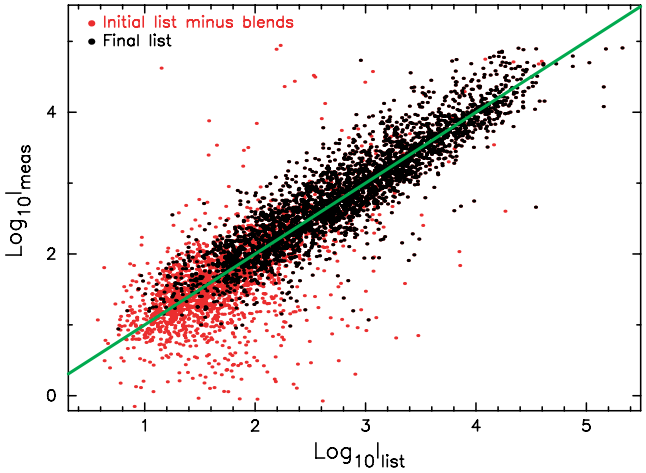

Figure 2. Lines from all categories placed on the UVES intensity scale. The grey/red points are lines from the initial LPWN list which satisfy the blending criterion defined in step (iv) of the ThAr selection algorithm. The black points are lines satisfying all selection criteria and constitute the final ThAr line-list. Here, $I_{\rm list}$ refers to the rescaled listed intensities and $I_{\rm meas}$ is the amplitude of the line measured from the UVES ThAr spectrum.

The velocity shift due to the blending line is therefore

$$\Delta v_{\rm c} \equiv \frac{\lambda_{\rm c} - \lambda_1}{\lambda_1} \approx \Delta v_{\rm sep} \frac{I_2/I_1}{1 + I_2/I_1}. \quad (2)$$

However, if the two lines are further apart and are partially resolved it is not clear how $\Delta\, v_{\rm c}$ will depend on $\Delta\, v_{\rm sep}$ and I_2/I_1. Fig. 3 (right-hand panel) shows the results of a numerical experiment where two blended lines are varied in relative intensity and separation and fitted with a single Gaussian with similar initial guesses as in step (ii). A by-eye fit to the contours of constant velocity shift gives the following relationship:

$$\frac{I_2}{I_1} \approx \left(\frac{\Delta v_{\rm sep}}{\Delta v_{\rm tol}} - 1\right)^{-1} + 0.1\left(\frac{\Delta v_{\rm sep}}{\sigma_{\rm v}}\right)^2 + 0.0012\left(\frac{\Delta v_{\rm sep}}{\sigma_{\rm v}}\right)^4. \quad (3)$$

The first term on the right-hand side is just the previous equation and applies when $\Delta v_{\rm sep}$ is small with respect to $\sigma_{\rm v} = (c/R)/2.355$ (c is the speed of light and c/R is the spectrograph's FWHM resolution). We therefore reject lines from the input line-list LPWN which have

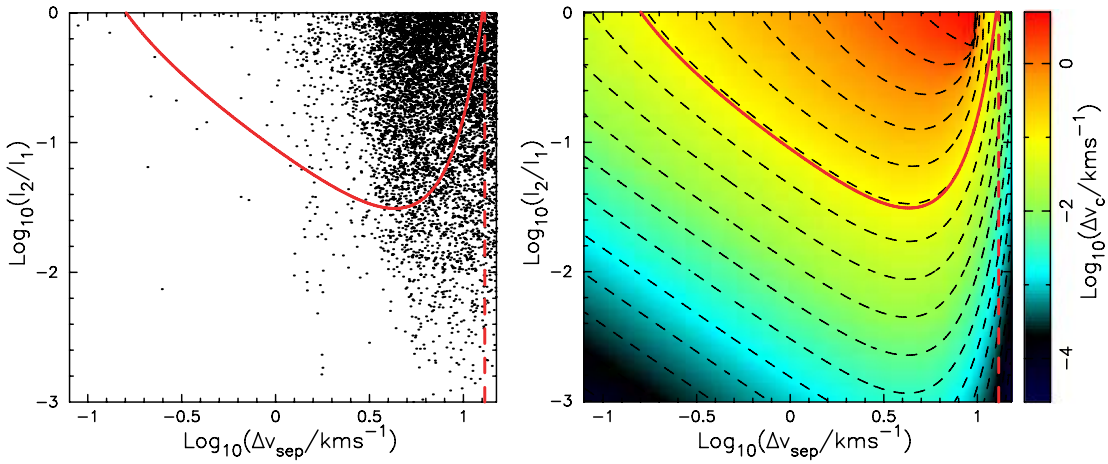

Figure 3. Removal of strongly blended lines. Right-hand panel: The shift in the centroid of a synthetic Gaussian due to blending with a weaker line. The black dashed lines are contours equally spaced in the logarithm of the shift. The solid grey/red line is a simple by-eye fit to these contours at a velocity tolerance of 40 m s^{-1} and $R = 43\,000$ (equation 3). All lines with blending lines more than 13 km s^{-1} away are safe from velocity shifts greater than 40 m s^{-1} and this is marked with the vertical dashed grey/red line. This figure is available in colour in the online version of the journal on *Synergy* and from http://www.ast.cam.ac.uk/mim/pub.html. Left-hand panel: Pairs of lines in the input line-list LPWN with the same solid and dashed grey/red lines from the right-hand panel.

blending lines within 13 km s^{-1} with relative intensities greater than that predicted by equation (3) to produce shifts greater than a tolerance of 40 m s^{-1} at $R = 43\,000$. This tolerance is similar to the overall wavelength calibration residuals achievable at a typical UVES resolution of $R = 43\,000$ with the final ThAr list.

(v) Removal of weak lines: If ThAr lines appear weak in the UVES lamp spectrum then the UVES pipeline's line-identification algorithm can fail or yield a false identification. The velocity precision available in very weak lines is also too small to be useful in calibrating the UVES wavelength scale. We therefore reject any lines with measured intensities (above the measured continuum) less than four times the measured continuum level.

(vi) FWHM selection: Any additional unknown features in the UVES ThAr spectrum can cause blending with the lines remaining after steps (iv) and (v) above. The next three steps aim to reject those lines which are effected in this way. The first of these steps is to remove lines whose widths are clearly inconsistent with the instrumental resolution, in this case $R \approx 70\,000$ or FWHM ≈ 4.3 km s^{-1}. Fig. 4 shows the distribution of FWHM for all lines which survive steps (iv) and (v) above. After visual inspection of the lines lying away from the main cluster around FWHM ~ 4.3 km s^{-1} it was clear that lines wider than $\sim$5.3 km s^{-1} or narrower than $\sim$3.5 km s^{-1} should be removed. Lines were too wide when they were blended with other unknown features or where saturation of the CCD occurred. Lines were typically fitted as very narrow when they were very weak.

(vii) High slope rejection: One of the improvements we made to the UVES pipeline was the addition of a continuum slope parameter to the Gaussian fitting of ThAr lines during wavelength calibration. If a line is close to a strong, previously unknown feature in the UVES ThAr spectrum then a large slope (relative to the line intensity) might be needed to fit the line properly. Since these unknown features probably vary with lamp conditions, lines fitted with large continuum slopes are best avoided when calibrating the wavelength scale. Fig. 5 shows the distribution of the absolute velocity difference, Δv_s, between two Gaussian fits – one made including the slope parameter, the other made with the slope fixed to zero – with continuum slope normalized by the line intensity. Visual inspection

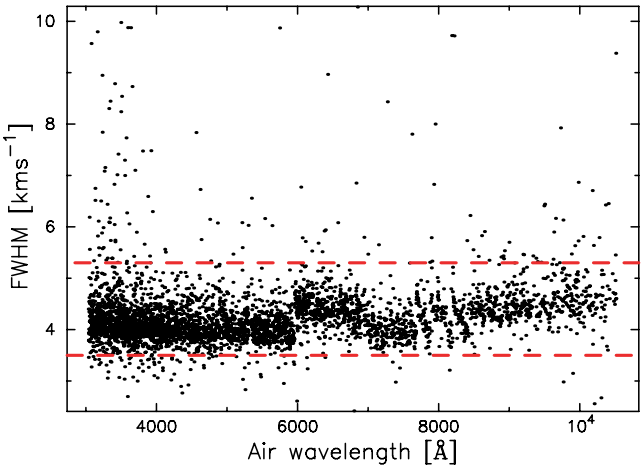

Figure 4. The FWHM distribution of the lines surviving steps (iv) and (v) in the selection algorithm. Most lines lie in a well-defined band around the expected FWHM of $\sim$4.3 m s^{-1}. The dashed lines indicate our selection criteria for suitable calibration lines. The structure seen in this band is due to slightly differing resolutions in the different exposures from different wavelength settings.

of lines with Δv_s greater than 80 m s^{-1} showed that some of them have large asymmetries which are due to close blends with unknown features. Therefore, all lines with $\Delta v_s \geqslant 80$ m s^{-1} are removed from the list at this stage.

(viii) Large residual rejection: As a final selection step we reject lines which are fitted at wavelengths at some variance to those expected from the input line-list LPWN. Since the ThAr line-list supplied with the UVES pipeline is known to contain several inaccuracies (see Section 1) we do not apply this criterion in the first pass through the selection algorithm. In the second pass we reject lines which are fitted at positions more than 0.25 km s^{-1} away from the expected position. In the third pass we reduce this parameter to 0.15 km s^{-1}, less than 1/10th of a pixel.

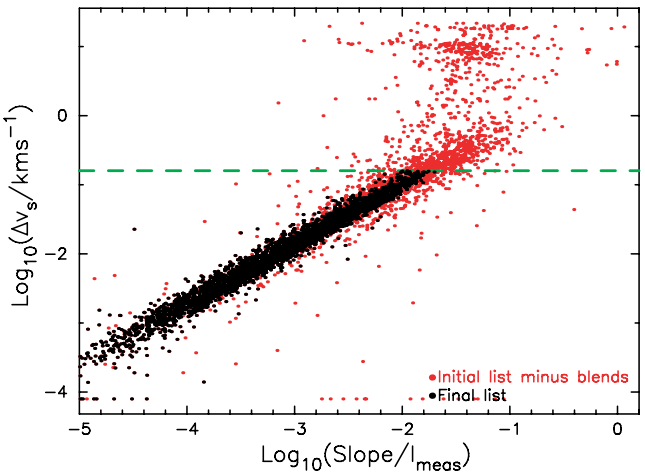

Figure 5. Distribution of the absolute velocity difference between the centroids of two Gaussian fits – one made including the slope parameter, the other made with the slope fixed to zero – versus the normalized continuum slope. A conservative cut is made at $\Delta v_s = 80\,\mathrm{m\,s^{-1}}$ to reject lines which might be effected by additional unknown features in the UVES ThAr spectrum.

4 FINAL THAR LINE-LIST

The ThAr line-list formed after the third pass through the selection algorithm, referred to hereafter as the final or new list, is shown in part in Table 1 and is available in its entirety from http://www.ast.cam.ac.uk/∼mim/pub.html and in the electronic version of this paper. In addition to an ASCII version, we also provide a version in a format which is readable by the UVES pipeline distributed by ESO.

The initial input list LPWN contains 13 903 lines while the final list contains just 3070. For comparison, the line-list supplied with the UVES pipeline contains 2387 lines over the wavelength range covered by UVES. So, although a large number of lines are rejected in the selection algorithm, there are certainly enough remaining lines to provide a reliable calibration of the UVES wavelength scale. Fig. 6 (left-hand panel) shows the distribution of lines with wavelength in bins which approximate the size of extracted UVES echelle orders. Compared to the initial input list, the distribution of lines is quite uniform. This is mainly because of the rejection of close blends and demonstrates why the LPWN catalogue should not be used without first selecting unblended and otherwise reliable lines. Of course, since LPWN contains so many lines, one can always achieve very low *formal* wavelength calibration residuals simply by defining a sufficiently small rejection threshold during the calibration. However, it is important to realize that with this approach many of the lines eventually used for calibration will actually be blends which will distort the wavelength solution.

Fig. 6 (left-hand panel) also shows that there are always more than ∼20 useful lines per UVES echelle order in the final list. This is enough to supply a robust wavelength calibration solution. Fig. 6 (right-hand panel) shows the distribution of lines at each step in the third pass through the selection algorithm. After the removal of close blends none of the subsequent steps removes lines in a strongly wavelength-dependent manner, as expected. Fig. 7 (left-hand panel) shows the contribution from Th, Ar and unidentified lines in the initial input list LPWN while Fig. 7 (right-hand panel) shows the composition of the final list. Note the strong decrease in the fraction of unidentified lines through the selection algorithm. This is because most of the unidentified lines are those newly discovered by LP07, many of which are quite weak and/or blended at the UVES resolution.

We have used the final list to calibrate the UVES ThAr spectrum a final time and the resulting spectrum is available at http://www.ast.cam.ac.uk/∼mim/pub.html and in the electronic version of this paper. In extracting and wavelength calibrating the spectrum with the modified UVES pipeline, we noted a dramatic improvement in the wavelength calibration residuals. To quantify this we wavelength calibrated the ThAr spectrum with two different input line-lists – the final list derived above and the selection of DCH98 for $R = 50\,000$ – with the same pipeline parameters. The one exception was the tolerance level for rejecting discrepant lines in the pipeline's wavelength calibration step. This was adjusted to optimize the calibration for each list; that is, a balance was sought between the number of calibration lines and rms residual per echelle order. The results are summarized in Fig. 8 which compares these two quantities for each echelle order in the 346- and 580-nm standard UVES wavelength settings.

Fig. 8 demonstrates that our new list provides a factor of $\gtrsim$3 improvement in the wavelength calibration residuals and, particularly for the 346-nm setting, provides more lines per echelle order on average. Note also the significant reduction in the number of orders – all at the bluest extreme of the 346-nm setting – which have less than 10 lines for calibration when using the new list. The 346- and 580-nm settings also illustrate the impact of the new LP07 ThAr catalogue on the residuals: the 346-nm setting covers wavelengths not covered by HARPS (spectra from which the LP07 catalogue was derived) while the 580-nm setting uses lines almost exclusively from LP07. The mean residual for the 346-nm setting is $36\,\mathrm{m\,s^{-1}}$ while that for the 580 setting is $28\,\mathrm{m\,s^{-1}}$ – a small but clear improvement due to the improved line wavelengths in LP07. Note that the mean residuals in the two settings are the same ($130\,\mathrm{m\,s^{-1}}$) when the spectra are calibrated with the DCH98 list.

Part of the motivation for this work was the various inaccuracies we noticed in the ThAr line-list distributed by ESO with the

Table 1. Excerpt from the final ThAr line-list for UVES. The complete table is available in the online version of this paper and at http://www.ast.cam.ac.uk/m̃im/pub.html. The first column is the wavenumber ($\lambda_{\rm vac} = 1 \times 10^8/\omega_0$), the second column is the air-wavelength computed from the vacuum wavelength, $\lambda_{\rm vac}$, using the Edlen (1966) formula for the dispersion of air at 15°C and atmospheric pressure (see Murphy et al. 2001a, for detailed discussion). The third column is the logarithm of the original listed intensity normalized to the (arbitrary) intensity scale of the UVES ThAr spectrum. The fourth and fifth columns provide the line identification when available. The final column identifies the source of the wavenumber and which intensity scale the line was originally on: 'L' indicates LP07, 'P' indicates PE83, 'N' indicates N73 while 'W' indicates W95 or W02. Unidentified lines are generally given element designations 'XX' and ionization levels of '0'. For unidentified lines in LP07 an ionization level '0' is given if the line appears in PE83 or '1' if LP07 claim the line was previously unknown.

ω_0 ($\mathrm{cm^{-1}}$)	$\lambda_{\rm air}$ (Å)	log 10 I	Line identity		Source
			Element	Ion	
26 473.6290	3776.271 162	3.299	Th	I	P
26 450.5761	3779.562 436	1.634	XX	0	P
26 426.4527	3783.012 697	2.576	Th	II	P
26 424.4709	3783.296 425	2.935	Th	II	P
26 415.5397	3784.575 599	2.242	XX	0	L
26 408.3869	3785.600 691	2.644	Th	II	L
26 402.9308	3786.383 000	2.653	Ar	II	L
26 392.1220	3787.933 732	1.813	Th	II	L

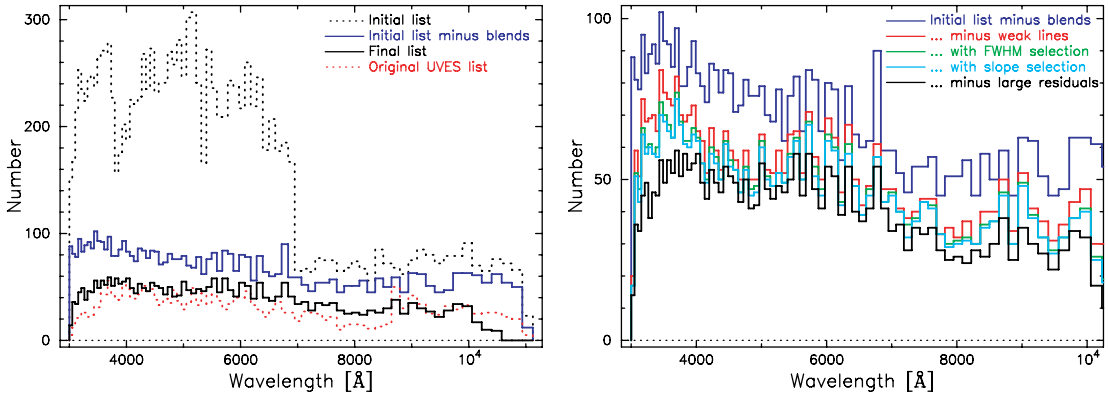

Figure 6. Histograms showing the expected number of lines per echelle order for different line-lists. Left-hand panel: Comparison of the initial line-list with the list after close blends have been removed. Also shown is a comparison of the final line-list with that provided with the UVES pipeline. Right-hand panel: The reduction of the line-list through the various selection stages.

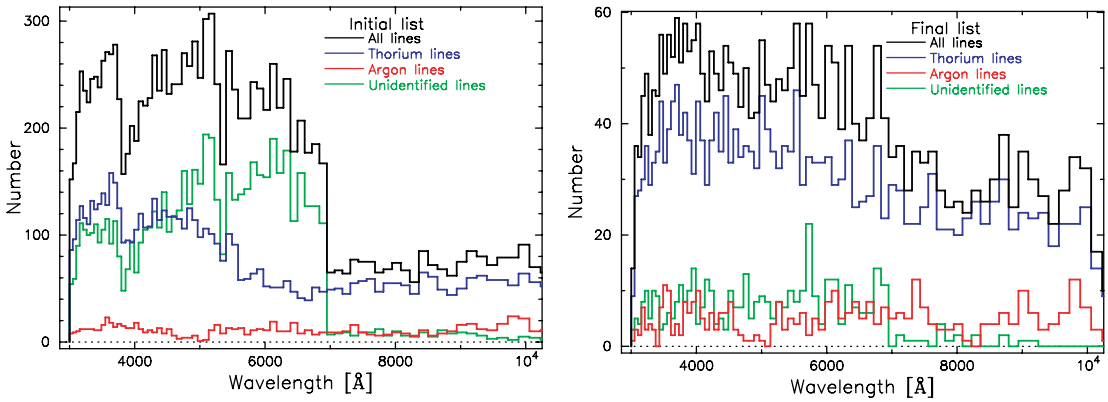

Figure 7. Histograms showing the contributions from Th, Ar and unidentified lines to the initial (left-hand panel) and final (right-hand panel) ThAr line-lists.

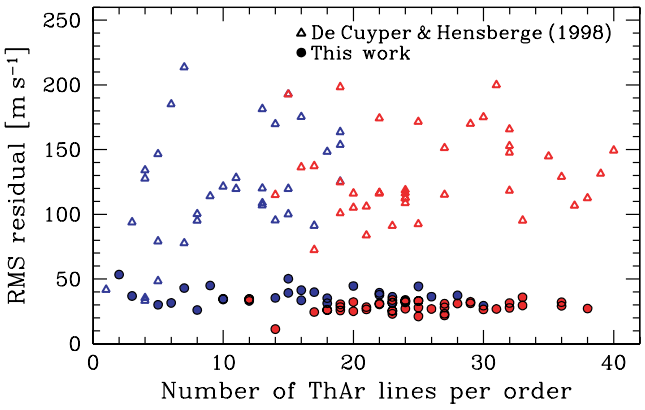

Figure 8. Improvement of the wavelength calibration solution using the new line-list (filled circles) over that achievable with the $R = 50\,000$ list from DCH98 (open triangles). The blue/darker points represent echelle orders from the 346-nm standard UVES wavelength setting while the red/lighter points are from the 580-nm setting. The calibration residuals for the 580-nm setting using our new list are slightly better than for the 346-nm setting due to the improved precision in the new LP07 ThAr atlas.

UVES pipeline (see Section 1). To investigate the effect these inaccuracies have on reduced spectra we have reduced the same raw ThAr exposures used above with the unmodified UVES pipeline and the ESO line-list. We then follow the line selection algorithm in Section 3.2 using a tolerance on the residuals of 0.3 km s^{-1} in step (viii). Using the LPWN line-list as input allows us to trace any distortions of the wavelength scale introduced by the inaccuracies in the ESO line-list and wavelength calibration procedure. The residuals between the Gaussian fit centroid wavelengths and the wavelengths listed in our final ThAr list derived above are plotted in Fig. 9. The mean residual shows strong, statistically significant variations with wavelength. The two most striking features are (i) the spike in the mean residual around 6300 Å which has a peak-to-peak amplitude of $\sim$75 m s^{-1} and (ii) the large-scale decrease in the mean residual from $\sim$0 m s^{-1} below 4500 Å to ~ -30 m s^{-1} over the range 5500–7000 Å and then the slow increase to $\sim +30$ m s^{-1} redwards of 7000 Å. These distortions of the wavelength scale have important consequences for several applications which have used pipeline-reduced UVES spectra. We illustrate one such application below.

5 IMPLICATIONS FOR CURRENT UVES CONSTRAINTS ON A VARYING FINE-STRUCTURE CONSTANT

Distortions of the wavelength scale of the magnitude and over the wavelength ranges just discussed are critically important to current UVES constraints on cosmological variations in the fine-structure constant, $\alpha_{\rm em}$, which employ the UVES pipeline and ESO line-list. The velocity shift, v, of a transition due to a small relative variation in $\alpha_{\rm em}$, $\Delta\alpha/\alpha \ll 1$, is determined by the q-coefficient for that

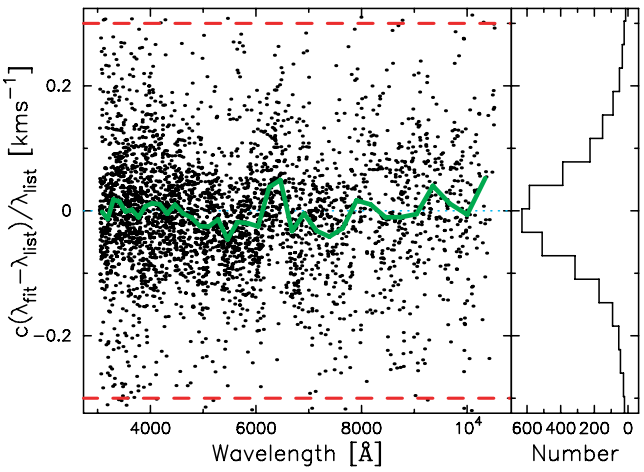

Figure 9. Residuals between the Gaussian fit centroid wavelengths measured from the ThAr spectrum (reduced using the unmodified UVES pipeline and ESO line-list), $\lambda_{\rm fit}$, and the wavelengths listed in the LPWN line-list compiled in this work, $\lambda_{\rm list}$. Note the structure in the residuals as a function of wavelength. The mean residual, in bins which approximate the size of two UVES echelle orders, is shown as a grey/green thick line. The typical error in the mean residual in each bin is ∼5–10 m s^{-1}. Thus, the strong variations from bin to bin and over longer wavelength ranges are statistically significant and indicate distortions of the wavelength scale introduced by the various inaccuracies in the ESO line-list and the UVES pipeline wavelength calibration procedures.

transition:

$$\omega_z \equiv \omega_0 + q\left[\left(\frac{\alpha_z}{\alpha_0}\right)^2 - 1\right] \quad \Rightarrow \quad \frac{v}{c} \approx -2\frac{\Delta\alpha}{\alpha}\frac{q}{\omega_0}, \qquad (4)$$

where ω_0 and ω_z are the rest frequencies in the laboratory and at redshift z, α_0 is the laboratory value of $\alpha_{\rm em}$ and α_z is the shifted value measured from an absorber at redshift z. The MM method is the comparison of measured velocity shifts from several transitions (with different q-coefficients) to compute the best-fitting $\Delta\alpha/\alpha$. Thus, the variation with wavelength in the magnitude and sign of the velocity shift in Fig. 9 will lead directly to spurious measurements of $\Delta\alpha/\alpha$ depending on (i) which transitions are utilized to compute $\Delta\alpha/\alpha$ and (ii) the redshift of the absorption system.

An example of this problem arises in the results of Chand et al. (2004) who studied 23 absorption systems and concentrated mainly on the Mg II λλ2796/2803 doublet and the five strong Fe II transitions redwards of 2340 Å. The single absorber which dominates their sample, with a quoted uncertainty on $\Delta\alpha/\alpha$ of just 0.1×10^{-5}, lies at redshift $z_{\rm abs} = 1.2433$. This places the three Fe II transitions used in their analysis at observed wavelengths between 5250 and 5340 Å and the Mg II doublet appears at around 6270 Å. Fig. 9 implies that a spurious velocity shift of 75 m s^{-1} between the Fe II and Mg II lines will be measured in this system. The three Fe II lines all have large, positive q-coefficients ∼1400 cm^{-1} while the Mg II doublet transitions both have very small q-coefficients ∼150 cm^{-1}. Equation (4) therefore implies that the 75 m s^{-1} velocity shift corresponds to a spurious $(\Delta\alpha/\alpha)_{\rm ThAr} \approx +0.4 \times 10^{-5}$, four times larger than the 1σ uncertainty quoted by Chand et al. (2004).

This example of converting the residuals in Fig. 9 into predictions of the systematic error in $\Delta\alpha/\alpha$ are easily generalized to any absorption redshift once a set of $n > 1$ transitions is specified. Fig. 10 shows two examples, one utilizing the Mg II doublet and the five redder Fe II transitions, the other using those five Fe II lines plus the Fe II λ1608 transition. At each step in redshift, the value of $(\Delta\alpha/\alpha)_{\rm ThAr}$ is calculated as follows: for each transition i, the seven ThAr lines which fall closest to its redshifted wavelength are identified and their mean residual, v_i (as defined in Fig. 9), is calculated. The error in each v_i is assumed to be the same and is set equal to the rms residual of all $7 \times n$ ThAr lines, divided by $\sqrt{7}$. A linear least-squares fit between the v_i values and the corresponding q-coefficients (equation 4)[6] then yields the best-fitting value of $(\Delta\alpha/\alpha)_{\rm ThAr}$ and its uncertainty.

The lower panel of Fig. 11 shows the values of $(\Delta\alpha/\alpha)_{\rm ThAr}$ for each of the 23 absorbers in the Chand et al. (2004) analysis. As described above, some absorbers are particularly sensitive to miscalibrations due to their redshift and the particular transitions used to determine $\Delta\alpha/\alpha$. However, for 18 of the 23 absorbers, $|(\Delta\alpha/\alpha)_{\rm ThAr}|$ is less than 0.2×10^{-5}. It is nevertheless important to asses the impact this has on the overall weighted mean value of $\Delta\alpha/\alpha$. The values of $\Delta\alpha/\alpha$, corrected by their respective $(\Delta\alpha/\alpha)_{\rm ThAr}$ values, are shown in the upper panel of Fig. 11. The errors bars are the quadrature addition of the original errors quoted by Chand et al. (2004) and the errors in $(\Delta\alpha/\alpha)_{\rm ThAr}$ shown in the lower panel. The weighted mean of the corrected values is $\Delta\alpha/\alpha = (-0.17 \pm 0.06) \times 10^{-5}$; a 2.5σ 'detection' of variation in $\alpha_{\rm em}$ compared to the null result of $\Delta\alpha/\alpha = (-0.06 \pm 0.06) \times 10^{-5}$ claimed by Chand et al. (2004). Note that the error bars on the $\Delta\alpha/\alpha$ values from Chand et al. (2004) plotted in Fig. 11 have been shown to be significant underestimates in Murphy, Webb & Flambaum (2007b,c). Thus, once larger, more appropriate error bars are used, the relative importance of wavelength calibration errors on the corrected Chand et al. (2004) result diminishes (Murphy et al. 2007b). Nevertheless, Figs 10 and 11 clearly demonstrate how the ESO line-list and the wavelength calibration procedure of the original UVES pipeline cause significant systematic effects in measurements of $\Delta\alpha/\alpha$ at the 0.1×10^{-5} precision level.

A similar analysis is presented by Chand et al. (2006) who cross-correlate two UVES ThAr spectra, one calibrated using the ESO line-list and the other calibrated using the line-list distributed by the National Optical Astronomy Observatory[7] (NOAO), to determine the distortions of the wavelength scale over the range 3100–6700 Å. They find very similar structures (in their fig. 7) to those seen in Fig. 9, including the sharp spike around 6300 Å. Chand et al. (2006) then test the effect these distortions would have on a single Mg/Fe II absorber at $z_{\rm abs} = 1.15$, using only the redder Fe II lines and the Mg II doublet.[8] Since these lines are all redshifted to wavelengths where the mean calibration residual is similar (i.e. between 5040 and 6030 Å) – falling just short of the spike around 6300 Å – it is not surprising to find little-to-no effect on $\Delta\alpha/\alpha$ at this redshift. Based on this single-redshift example, Chand et al. (2006) claim that current UVES constraints on $\Delta\alpha/\alpha$ should be fairly immune to any problems introduced by the ESO line-list and (unmodified) UVES pipeline wavelength calibration procedures. As demonstrated in the specific examples above and in the more general cases illustrated in Figs 10 and 11, such a simplistic extrapolation to other redshifts significantly underestimates the systematic errors involved.

[6] Although equation (4) formally has zero y-intercept, the fit between the v_i and q values must contain the y-intercept as a free parameter, to be determined simultaneously with $(\Delta\alpha/\alpha)_{\rm ThAr}$. This amounts to determining the best-fitting redshift of the set of the ThAr lines, mimicking the situation in the quasar spectra where one must determine the best-fitting $\Delta\alpha/\alpha$ and redshift simultaneously.

[7] http://www.noao.edu/kpno/specatlas/thar/thar.html

[8] Chand et al. (2006) do not consider the Fe II λ1608 line in this test despite the fact that their analysis of the real absorber relies most heavily on this single transition.

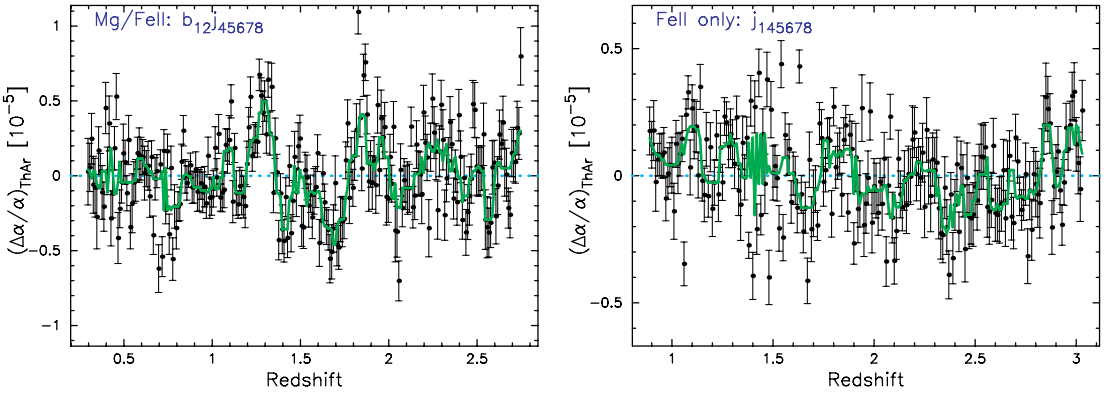

Figure 10. The spurious value of $\Delta\alpha/\alpha$ implied by the residuals in Fig. 9 $(\Delta\alpha/\alpha)_{\rm ThAr}$, as a function of redshift, assuming two different sets of transitions. The left-hand panel utilizes the Mg II $\lambda\lambda$2796/2803 doublet and Fe II λ2344, 2374, 2382, 2586 and 2600 lines. The right-hand panel uses the same Fe II lines plus the Fe II λ1608 transition. The solid grey/green line shows a running median of $(\Delta\alpha/\alpha)_{\rm ThAr}$ over seven redshift bins. The redshift bins are $\Delta\, z = 0.01$ wide. If one had measured a value of $\Delta\alpha/\alpha$ from an absorber at a given redshift in a spectrum reduced with the unmodified UVES pipeline and calibrated using the ESO line-list, one would have to subtract the value of $(\Delta\alpha/\alpha)_{\rm ThAr}$ at that redshift to derive a more reliable estimate.

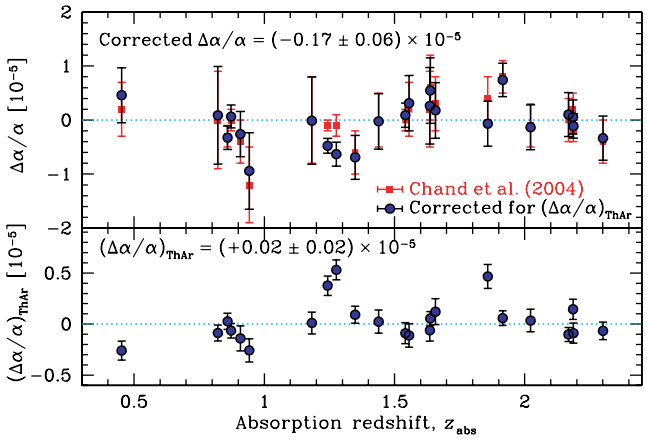

Figure 11. Effect of wavelength calibration errors on the $\Delta\alpha/\alpha$ values of Chand et al. (2004). The lower panel gives the systematic error $(\Delta\alpha/\alpha)_{\rm ThAr}$ for each absorber while the upper panel shows the original $\Delta\alpha/\alpha$ values (red/grey squares) corrected by their respective $(\Delta\alpha/\alpha)_{\rm ThAr}$ values (solid circles). Even though the weighted mean calibration error is just $(\Delta\alpha/\alpha)_{\rm ThAr} = (+0.02 \pm 0.02) \times 10^{-5}$, the fact that some of the (apparently) most precise $\Delta\alpha/\alpha$ values have large corrections means that the corrected weighted mean $\Delta\alpha/\alpha$ shifts significantly to $\Delta\alpha/\alpha = (-0.17 \pm 0.06) \times 10^{-5}$.

Finally, note that in Murphy et al. (2001a) and Murphy et al. (2003) we carried out a similar analysis on the Keck/HIRES spectra which provided our previous constraints on $\Delta\alpha/\alpha$. The wavelength calibration employed the NOAO ThAr line-list discussed above. In those works we found no such structures like those seen in Fig. 10. Thus, although the current UVES constraints on $\Delta\alpha/\alpha$ have been adversely affected by the ESO line-list, such a problem does not generally exist for HIRES constraints to any significant degree.

6 CONCLUSIONS

We have implemented a simple iterative algorithm to select ThAr lines for use in calibrating echelle spectrographs. The algorithm combines the expected line properties (e.g. degree of blending), based on the input line-list, with properties of the ThAr spectrum observed on the spectrograph of interest (e.g. resolution, relative line intensities, etc.). We emphasize that although this paper has focused on the application of this algorithm to VLT/UVES spectra, the algorithm can be applied to any other spectrograph; all that is required is a ThAr spectrum taken on that spectrograph and a reduction code which allows repeatable wavelength calibration with different ThAr line-lists.

Using the most recent and reliable ThAr laboratory wavelengths, including that of LP07, we have produced a new ThAr line-list which, we argue, should be used to calibrate UVES spectra in preference to the list distributed by ESO. The main advantages of the former over the latter are: (i) more homogeneous input line catalogues with mutually consistent wavelength scales; (ii) more accurate and precise laboratory wavelengths; (iii) only unblended lines appear in the final list and (iv) only lines which are *observed* to be useful in UVES spectra are included. Indeed, the wavelength calibration residuals achieved using the new UVES line-list (rms $\sim 35\,{\rm m\,s^{-1}}$) are more than a factor of 3 better than those achieved with the ESO or DCH98 list (rms $\sim 130\,{\rm m\,s^{-1}}$) – see Fig. 8. An assumption one makes in using our new line-list to calibrate UVES spectra is that the relative line intensities (i.e. lamp conditions like pressure, current, etc.) are similar to those in the sample UVES ThAr spectra used in our selection algorithm. However, ideally, the selection algorithm should be included in the wavelength calibration procedure itself, thus producing the best selection of ThAr lines for each individual ThAr exposure being reduced.

The new line-list has been used to probe distortions of the wavelength scale introduced into UVES spectra which were originally wavelength calibrated with the ESO line-list. The distortions include sharp, short-range corrugations with peak-to-peak amplitude up to $\sim$75 m s^{-1} and longer range variations between $+30\,{\rm m\,s^{-1}}$ and $-30\,{\rm m\,s^{-1}}$ (Fig. 9). These distortions have serious implications in the context of current UVES estimates of possible variations in the fine-structure constant, especially those of Chand et al. (2004) – see Figs 10 and 11. For example, if one employs the common Mg/Fe II combination of transitions to derive $\Delta\alpha/\alpha$ then the errors in the ESO line-list cause a spurious value of $(\Delta\alpha/\alpha)_{\rm ThAr} \approx +0.4 \times 10^{-5}$ for absorption redshifts $1.22 \lesssim z_{\rm abs} \lesssim 1.35$ and $(\Delta\alpha/\alpha)_{\rm ThAr} \approx -0.3 \times 10^{-5}$ for $1.38 \lesssim z_{\rm abs} \lesssim 1.75$. Although Chand et al. (2004) claim an overall precision in $\Delta\alpha/\alpha$ of 0.06×10^{-5} from 23 Mg/Fe II absorbers (but see Murphy et al. 2007b,c), a single absorber at $z_{\rm abs} = 1.2433$ strongly dominates their sample with an individual

error on $\Delta\alpha/\alpha$ of 0.1×10^{-5}. However, at this redshift, and considering which transitions are used to derive $\Delta\alpha/\alpha$ in this system, we find that a spurious systematic shift of $(\Delta\alpha/\alpha)_{\rm ThAr} \approx +0.4 \times 10^{-5}$ has affected this system. Once such wavelength calibration corrections are applied to the entire sample, the null result of $\Delta\alpha/\alpha = (-0.06 \pm 0.06) \times 10^{-5}$ claimed by Chand et al. (2004) becomes $\Delta\alpha/\alpha = (-0.17 \pm 0.06) \times 10^{-5}$ – a 2.5σ 'detection'. The new ThAr line-list we present here should aid in avoiding such important yet elementary errors in future analyses of UVES spectra.

ACKNOWLEDGMENTS

We thank R. Engleman and W. Whaling for detailed discussions about the Th and Ar line-lists, respectively, and for providing the lists in electronic form. R. Fear of Cathodeon, manufacturer of ThAr hollow cathode lamps, also provided helpful information concerning the operating conditions of such lamps. MTM thanks PPARC for an Advanced Fellowship at the IoA.

REFERENCES

Breckinridge J. B., Pierce A. K., Stoll C. P., 1975, ApJS, 29, 97
Chand H., Srianand R., Petitjean P., Aracil B., 2004, A&A, 417, 853
Chand H., Srianand R., Petitjean P., Aracil B., Quast R., Reimers D., 2006, A&A, 451, 45
De Cuyper J.-P., Hensberge H., 1998, A&AS, 128, 409 (DCH98)
Dzuba V. A., Flambaum V. V., Webb J. K., 1999, Phys. Rev. Lett., 82, 888
Edlen B., 1966, Metrologia, 2, 71
Giacchetti A., Stanley R. W., Zalubas R., 1970, J. Opt. Soc. Am., 60, 474
Levshakov S. A., Centurión M., Molaro P., D'Odorico S., Reimers D., Quast R., Pollmann M., 2006, A&A, 449, 879
Lovis C., Pepe F. 2007, A&A, in press (astro-ph/0703412) (LP07)
Marcy G. W., Butler R. P., 1992, PASP, 104, 270
Meggers W. F., 1957, in Oosterhoff P. T., ed., Trans. IAU Vol. 9, Proceedings of the Ninth General Assembly. Cambridge Univ. Press, Cambridge, p. 225
Minnhagen L., 1973, J. Opt. Soc. Am., 63, 1185
Murphy M. T., Webb J. K., Flambaum V. V., Churchill C. W., Prochaska J. X., 2001a, MNRAS, 327, 1223
Murphy M. T., Webb J. K., Flambaum V. V., Dzuba V. A., Churchill C. W., Prochaska J. X., Barrow J. D., Wolfe A. M., 2001b, MNRAS, 327, 1208
Murphy M. T., Webb J. K., Flambaum V. V., 2003, MNRAS, 345, 609
Murphy M. T., Flambaum V. V., Webb J. K., Dzuba V. V., Prochaska J. X., Wolfe A. M., 2004, Lecture Notes Phys., 648, 131
Murphy M. T. et al. 2007a, MNRAS, in press (astro-ph/0703622)
Murphy M. T., Webb J. K., Flambaum V. V. 2007b, Phys. Rev. Lett., submitted, preprint (astro-ph/0612407)
Murphy M. T., Webb J. K., Flambaum V. V., 2007c, in Pasquini L., Romaniello M., Santos N. C., Correia A., eds, Precision Spectroscopy in Astrophysics. Springer-Verlag, Berlin, Germany, preprint (astro-ph/0611080)
Norlén G., 1973, Phys. Scr., 8, 249 (N73)
Palmer B. A., Engleman R., 1983, Technical Report, Atlas of the Thorium Spectrum. Los Alamos National Laboratory, NM, USA (PE83)
Rosman K. J. R., Taylor P. D. P., 1998, J. Phys. Chem. Ref. Data, 27, 1275
Webb J. K., Flambaum V. V., Churchill C. W., Drinkwater M. J., Barrow J. D., 1999, Phys. Rev. Lett., 82, 884
Webb J. K., Murphy M. T., Flambaum V. V., Dzuba V. A., Barrow J. D., Churchill C. W., Prochaska J. X., Wolfe A. M., 2001, Phys. Rev. Lett., 87, 091301
Whaling W., Anderson W. H. C., Carle M. T., Brault J. W., Zarem H. A., 1995, J. Quant. Spectrosc. Radiat. Transfer, 53, 1 (W95)
Whaling W., Anderson W. H. C., Carle M. T., Brault J. W., Zarem H. A., 2002, J. Res. Natl. Inst. Standards Technol., 107, 149 (W02)

SUPPLEMENTARY MATERIAL

The following supplementary material is available for this article:

Table 1. The final ThAr line-list for UVES. In addition to an ASCII version, we also provide a version in a format which is readable by the UVES pipeline distributed by ESO.

This material is available as part of the online article from: http://www.blackwell-synergy.com/doi/abs/10.1111/j.1365-2966.2007.11768.x (this link will take you to the article abstract).

Please note: Blackwell Publishing are not responsible for the content or functionality of any supplementary materials supplied by the authors. Any queries (other than missing material) should be directed to the corresponding author for the article.

This paper has been typeset from a TEX/LATEX file prepared by the author.